A STUDY OF SIDELOBE REDUCTION FOR LIMITED DIFFRACTION BEAMS

Jian-yu Lu and James F. Greenleaf

Biodynamics Research Unit, Department of Physiology and Biophysics,
Mayo Clinic and Foundation, Rochester, MN 55905

ABSTRACT

Limited diffraction beams have a large depth of field and are approximately depth-independent, even if they are produced with a finite aperture. Therefore, they may have applications in medical imaging, tissue characterization, nondestructive evaluation of materials, as well as other physical branches such as optics and electromagnetics. However, limited diffraction beams have larger sidelobes than those of conventional beams at their focuses. A method has been proposed for reducing the sidelobes of limited diffraction beams at the expense of frame rate. In this paper, we study the efficacy of the method when stepwise aperture weighting functions are used to produce the beams. Results show that the method works well with a transducer of only 14 rings and 16 sectors. The transducer has a 25 mm diameter and 3.5 MHz central frequency, and can produce a pulse-echo response that maintains a -6-dB mainlobe width of about 1.83 mm over a depth of field of about 150 mm.

I. INTRODUCTION

Limited diffraction beams are a special class of solutions to the isotropic-homogeneous wave equation. They would propagate to infinite distance without spreading, provided that they were produced with an infinite aperture and energy [1]. Even if produced with a finite aperture, these beams have a large depth of field and approximate depth-independent property [1]. Because of these properties, limited diffraction beams could have applications in medical imaging [2,3], tissue characterization [4], nondestructive evaluation of materials [5], color Doppler imaging [6], and other wave related physical branches such as optics [7] and electromagnetics [8–9].

Although limited diffraction beams have a large depth of field, they have higher sidelobes than those of conventional beams at their focuses. Sidelobes may lower contrast in medical imaging affecting the detection of low scattering objects such as small cysts. Sidelobes also increase the effective sampling volume in tissue characterization. In addition, sidelobes are a source of multiple scattering in nondestructive evaluation of materials.

We have developed a summation-subtraction method that reduces dramatically the sidelobes of limited diffraction pulse-echo systems (limited diffraction beams are used in both transmission and reception) at the expense of frame rate [10]. The price paid for the sidelobe reduction of limited diffraction pulse-echo systems is similar to that for a conventional system in which a montage process is used to increase the depth of field while maintaining low sidelobes and thus also lowing the frame rate. In this paper, we study the efficacy of the summation-subtraction method when stepwise aperture weightings are used to produce the beams. A transducer that could be used with the method is described.

II. THE SUMMATION-SUBTRACTION METHOD

Two examples of limited diffraction beams, the Bessel beam [1] and X wave [11,12], will be studied for their sidelobe reduction. Zeroth-order limited diffraction beams have both a mainlobe and high sidelobes, and second-order beams do not have the mainlobe but similar sidelobes. Therefore, subtraction of A-lines obtained with beams of different orders may result in a dramatic sidelobe reduction. If we assume that biological soft tissues are composed of point scatterers that are distributed randomly in the half space, $z > 0$, and multiple scattering among the scatters is negligible, the A-line produced by a Bessel pulse-echo system after sidelobe reduction is given by [10]

$$\begin{aligned} e(t) &= e_{J_0}(t) - \left[e_{J_2}(t)|_{\phi_0=0} + e_{J_2}(t)|_{\phi_0=\pi/4}\right] \\ &= 4\pi^2 \int_{-\infty}^{\infty} r\,dr \int_{-\pi}^{\pi} d\phi \int_{0}^{\infty} dz A(r,\phi,z) \\ &\cdot \left[J_0^2(\alpha r) - J_2^2(\alpha r)\right] \mathcal{F}^{-1}\left\{T^2(\omega) e^{i2\beta z}\right\}, \end{aligned} \tag{1}$$

where $e_{J_2}(t)|_{\phi_0=0}$ and $e_{J_2}(t)|_{\phi_0=\pi/4}$ are A-lines obtained with second-order Bessel beams that are rotated $\pi/4$ relative to each other, ϕ_0 is an initial angle of the second-order Bessel beams, $e_{J_0}(t)$ is an A-line obtained with a zeroth-order Bessel beam, $A(r,\phi,z)$ denotes the reflection coefficients of scatterers and is a function of the spatial coordinates (in cylindrical coordinates), $\vec{r} = (r,\phi,z)$, $J_0(\cdot)$ and $J_2(\cdot)$ are the zeroth- and second-order Bessel functions of the first kind, $\mathcal{F}^{-1}$ denotes the inverse Fourier transform with respect to the angular frequency, ω, $T^2(\omega)$ is a combined transmitting and receiving transfer function of the transducer, and $\beta = \sqrt{(\omega/c)^2 - \alpha^2}$, where c is the speed of sound (assumed to be 1500 m/s)

1051-0117/93/0000-1077 $4.00

in biological soft tissues, and α is a scaling factor of the Bessel functions. Similarly, the A-line obtained with an X wave pulse-echo system after the sidelobe reduction is given by [10]

$$e(t) = e_{X_0}(t) - \left[e_{X_2}(t)|_{\phi_0=0} + e_{X_2}(t)|_{\phi_0=\pi/4}\right]$$
$$= \frac{4\pi^2}{c^2} \int_{-\infty}^{\infty} r dr \int_{-\pi}^{\pi} d\phi \int_{0}^{\infty} dz A(r,\phi,z)$$
$$\cdot \mathcal{F}^{-1}\left\{G(\omega,r,\zeta)B^2\left(\frac{\omega}{c}\right)H^2\left(\frac{\omega}{c}\right)e^{-2\frac{\omega}{c}a_0}e^{i2\frac{\omega}{c}z\cos\zeta}\right\}, \quad (2)$$

where $G(\omega,r,\zeta) = J_0^2\left(\frac{\omega}{c}r\sin\zeta\right) - J_2^2\left(\frac{\omega}{c}r\sin\zeta\right)$, $e_{X_0}(t)$ and $e_{X_2}(t)$ are the A-lines obtained with the zeroth- and second-order X waves [11,12], respectively, $H\left(\frac{\omega}{c}\right) = \begin{cases} 1, & \omega \geq 0 \\ 0, & \omega < 0 \end{cases}$ is the Heaviside step function [13], $B^2(\omega/c) = T^2(\omega)$ is the combined transmitting and receiving transfer function of the transducer, a_0 is a parameter that controls the high-frequency component of the X waves and ζ is the Axicon angle.

From Eqs. (1) and (2) we see that $\left|J_0^2(\cdot) - J_2^2(\cdot)\right|$ is much smaller than $J_0^2(\cdot)$ except in the mainlobe because both $J_0^2(\cdot)$ and $J_2^2(\cdot)$ have similar sidelobes but $J_2^2(\cdot)$ does not have a mainlobe. Therefore, the scatterers in the region where $\left|J_0^2(\cdot) - J_2^2(\cdot)\right|$ is small do not have significant contributions to the A-lines, $e(t)$.

We now explain the sidelobe reduction in Fig. 1. If there is only one point scatterer in the space, $\vec{r}_0$, or $A(r,\phi,z) = \delta(\vec{r} - \vec{r}_0)$, Eqs. (1) and (2) represent the point spread functions of pulse-echo systems. The point spread functions in a transverse plane of the zeroth-order, second-order before rotation, and second-order after $\pi/4$ rotation beams are shown in Panels (1), (2), and (3), respectively. The summation of Panels (2) and (3) is shown in Panel (4), and the subtraction of Panel (4) from Panel (1) results in a significant sidelobe reduction (Panel (5)). In Fig. 1, we assume that α = 1202.45 m^{-1}, and the central wavelength is 0.6 mm (2.5 MHz central frequency).

The point spread functions in Fig. 1 are plotted along their diameters (Fig. 2). The parameters in Fig. 2 are as follows: α = 1217.51 m^{-1}, and the central wavelength is 0.429 mm (3.5 MHz central frequency).

III. STEPWISE APERTURE WEIGHTING IN ANGULAR DIRECTION

Eqs. (1) and (2) are formulas for sidelobe reduction of limited diffraction beams that are produced with a transducer of an infinite aperture. The formulas for the sidelobe reduction with a finite aperture transducer can be obtained with the Rayleigh-Sommerfeld diffraction formula [10, 14]. In this section, we study the influence on the sidelobe reduction of limited diffraction beams produced with a 25 mm diameter transducer of stepwise aperture weightings in the angular direction, ϕ, and exact aperture weightings in the radial direction, r. The transmitting or receiving transfer functions, $T(\omega)$ and $B(\omega/c)$ in Eqs. (1) and (2), of the transducer are assumed to be a Blackman window function [15] that peaked at 3.5 MHz with a relative bandwidth of about 81% (−6-dB bandwidth over the central frequency). The speed of sound, c, is assumed to be 1500 m/s giving a central wavelength of about 0.429 mm.

Line plots along the diameters of the point spread functions of a Bessel pulse-echo system before and after the sidelobe reduction are shown in Fig. 3. The transducer is divided into sectors to apply the stepwise aperture weightings to produce the second-order beams. The sidelobes are reduced as the number of sectors is increased. The scaling factor of the Bessel beams is α = 1217.51 m^{-1} and the depth of field is about 150.0 mm [1]. Line plots along the diameters of the point spread functions of an X wave pulse-echo system before and after the sidelobe reduction are shown in Fig. 4. The parameters of the X wave are as follows: a_0 = 0.05 mm, ζ = 4.75°, and the depth of field [11] is about 150.4 mm. The maximum sidelobes in the 2π angle of ϕ are plotted versus the radial distance (Fig. 5), when a 3.5 MHz tone burst is used to drive the Bessel pulse-echo system in Fig. 3.

IV. STEPWISE APERTURE WEIGHTING IN BOTH RADIAL AND ANGULAR DIRECTIONS

In this section, we study the sidelobe reduction when stepwise aperture weightings are applied to both the radial and angular directions. Along the radial direction, r, the transducer is divided into 14 rings. The positions of the rings are determined by the lobes of the absolute values of the Bessel function, $|J_0(\alpha r)|$. With the above parameters (α = 1217.51 m^{-1} and the diameter of the transducer of 25 mm), $|J_0(\alpha r)|$ has about five lobes (Fig. 2). The first lobe is divided into 2 rings of equal distance and each of the rest is divided into 3 rings of equal distance. Results of the sidelobe reduction for the 14-ring transducer of different numbers of sectors are shown in Figs. 6 to 8 that correspond to Figs. 3 to 5, respectively. There is little difference between these two groups of plots. Again, we see that sidelobes are reduced as the number of the sectors is increased. However, when the number of the sectors is greater than 16, the reduction of the sidelobes is diminished while number of the transducer elements and thus the system complexity may be increased dramatically.

V. A PROPOSED TRANSDUCER

From the above studies, we may design a transducer that can produce both the zeroth- and higher-order limited diffraction beams to reduce the sidelobes of limited diffraction pulse-echo systems with the summation-subtraction method (Fig. 10). The transducer is composed of 14 rings as described in the last section and the rings are divided into 16 sectors. The total number of elements of the transducer is 209 (the center element is not divided into sectors and is only used for producing zeroth-order beams). Because the limited diffraction beams are symmetric about the center of the transducer in any opposite sectors, the number of wires required to drive the transducer is only 105 (the remaining elements are connected inside the transducer). To reduce acoustic cross talk, 1–3 ceramics/polymer composite material may be used to construct the transducer. The transducer proposed in Fig. 10 has the same structure as that we constructed and used with a wobbler for real-time medical imaging [16], except that the former is divided into 16 sectors.

VI. DISCUSSION

A. Frame Rate. The price paid for sidelobe reduction of limited diffraction beams with the summation-subtraction method is that the frame rate is reduced to 1/3. More higher-order limited diffraction beams can be used to further reduce the sidelobes [10, 17], which lowers further the frame rate. Low frame rate causes distortions when imaging fast moving objects such as the heart.

B. Dynamic Range. Because A-lines are subtracted in the summation-subtraction method, large contributions from sidelobes may be subtracted. This reduces the dynamic range of the signals after the subtraction and thus lowers the signal-to-noise ratio.

C. Motion Artifacts. Apparently, the summation-subtraction method is sensitive to the motion of objects or transducer. However, if the time between the adjacent A-lines for the summation and subtraction is short, the influence of motion will be small. Steering limited diffraction beams with a two-dimensional phased array [18] may eliminate the motion of the transducer.

D. System Complexity. Like the montage process for increasing the depth of field while maintaining low sidelobes in conventional scanners, the summation-subtraction method for reducing the sidelobes of limited diffraction beams also increases the system complexity. However, limited diffraction beams continue to have an approximate depth-independent property over a large depth of field after the sidelobe reduction.

E. Other Methods. Because limited diffraction beams have an approximately depth-independent point spread function within their deep depth of field, image restoration methods such as the Wiener filtering may be used to enhance resolutions as well as suppress the sidelobes [19, 20].

VII. CONCLUSION

The summation-subtraction method for reducing sidelobes of limited diffraction beams works not only with an exactly weighted finite aperture transducer [10], but with transducers weighted approximately with a stepwise function. Results from the computer simulations show that with a 3.5 MHz central frequency (0.429 mm central wavelength), 14-ring and 16-sector transducer (Fig. 10), the sidelobes of a limited diffraction pulse-echo system whose point spread function has a −6-dB mainlobe width of about 1.83 mm can be reduced dramatically over a large depth of field of about 150 mm, although the frame rate is reduced to 1/3.

VIII. ACKNOWLEDGMENTS

The authors appreciate the secretarial assistance of Elaine C. Quarve. This work was supported in part by grants CA 43920 and CA 54212 from the National Institutes of Health.

IX. REFERENCES

1. J. Durnin, J. J. Miceli, Jr., and J. H. Eberly, "Diffraction-free beams," Phys. Rev. Lett. 58(15):1499–1501, April 13, 1987.
2. Jian-yu Lu and J. F. Greenleaf, "Ultrasonic nondiffracting transducer for medical imaging," IEEE Trans. Ultrason. Ferroelec. Freq. Contr. 37(5):438–447, Sept., 1990.
3. Jian-yu Lu and J. F. Greenleaf, "Pulse-echo imaging using a nondiffracting beam transducer," Ultrason. Med. Biol. 17(3):265–281, May, 1991.
4. Jian-yu Lu and J. F. Greenleaf, "Evaluation of a nondiffracting transducer for tissue characterization," IEEE 1990 Ultrason. Symp. Proc. 90CH2938-9 2:795–798, 1990.
5. Jian-yu Lu and J. F. Greenleaf, "Producing deep depth of field and depth-independent resolution in NDE with limited diffraction beams," Ultrason. Imag. 15(2):134–149, April, 1993.
6. P. A. Magnin, "A review of Doppler flow mapping techniques," IEEE 1987 Ultrason. Symp. Proc. 87CH2492-7, 2:969–977, 1987.
7. J. Ojeda-Castaneda and A. Noyola-Iglesias, "Nondiffracting wavefields in grin and free-space," Microwave and Optical Tech. Lett. 3(12):430–433, Dec. 12, 1990.
8. J. N. Brittingham, "Focus wave modes in homogeneous Maxwell's equations: transverse electric mode," J. Appl. Phys. 54(3):1179–1189, 1983.
9. R. W. Ziolkowski, D. K. Lewis, and B. D. Cook, "Evidence of localized wave transmission," Phys. Rev. Lett. 62(2):147–150, Jan. 9, 1989.

10. Jian-yu Lu and J. F. Greenleaf, "Sidelobe reduction for limited diffraction pulse-echo systems," IEEE Trans. Ultrason. Ferroelec., Freq. Contr. 40(6) (to be published in Nov., 1993).
11. Jian-yu Lu and J. F. Greenleaf, "Nondiffracting X waves—exact solutions to free-space scalar wave equation and their finite aperture realizations," IEEE Trans. Ultrason. Ferroelec. Freq. Contr. 39(1):19–31, Jan., 1992.
12. Jian-yu Lu and J. F. Greenleaf, "Experimental verification of nondiffracting X waves," IEEE Trans. Ultrason. Ferroelec. Freq. Contr. 39(3):441–446, May, 1992.
13. R. Bracewell, *The Fourier Transform and its Applications*. New York, NY: McGraw-Hill Book Company, 1965, chs. 4 and 6.
14. J. W. Goodman, *Introduction to Fourier Optics*. New York, NY: McGraw-Hill, 1968, chs. 2–4.
15. A. V. Oppenheim and R. W. Schafer, *Digital Signal Processing*, Englewood Cliffs, NJ: Prentice-Hall, Inc., 1975, ch. 5.
16. Jian-yu Lu, T. K. Song, R. R. Kinnick, and J. F. Greenleaf, "*In vitro* and *in vivo* real-time imaging with ultrasonic limited diffraction beams," IEEE Trans. Med. Imag. 12(4) (to be published in Dec., 1993).
17. J. P. Wild, "A new method of image formation with annular apertures and application in radio astronomy," Proc. Royal Soc. A, 286:499–509, 1965.
18. Jian-yu Lu and J. F. Greenleaf, "Steering of limited diffraction beams with a two-dimensional array transducer," IEEE 1992 Ultrason. Symp. Proc. 92CH3118-7, 1:603–607, 1992.
19. Jian-yu Lu and J. F. Greenleaf, "Diffraction-limited beams and their applications for ultrasonic imaging and tissue characterization," in *New Developments in Ultrasonic Transducers and Transducer Systems*, F. L. Lizzi, Editor, Proc. SPIE 1733:92–119, 1992.
20. A. Rosenfeld and A. C. Kak, *Digital Picture Processing*, New York: Academic Press, 1982.

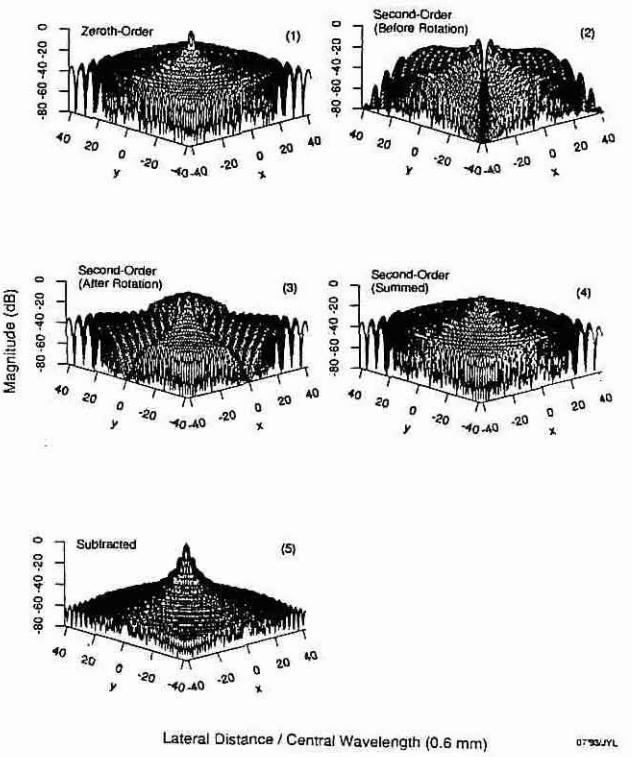

Fig. 1 Point spread functions of a Bessel beam pulse-echo system in a transverse plane that is parallel to the transducer surface: (1) zeroth-order system, (2) second-order system before rotation, (3) second-order system after $\pi/4$ rotation around the beam axis, (4) summation of the two point spread functions of the second-order systems, and (5) absolute values of the subtraction between Panels (4) and (1). [Reproduced with permission from Fig. 2 in Reference [10]].

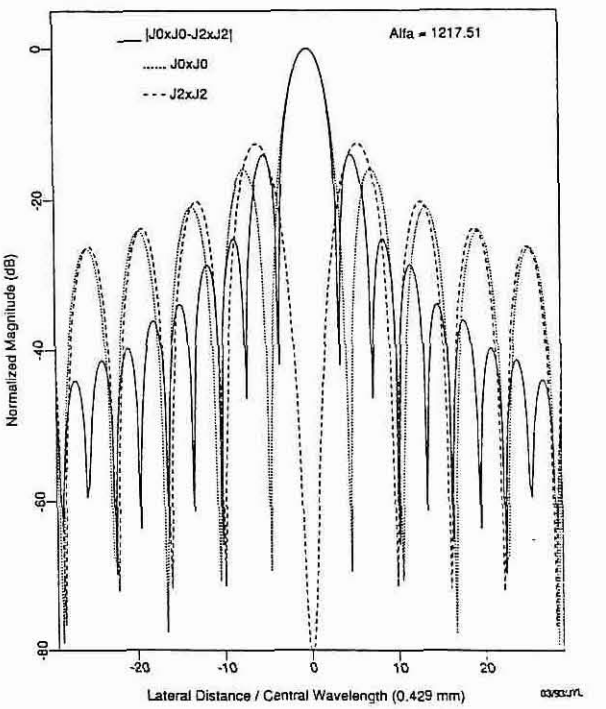

Fig. 2 Sidelobes of a Bessel pulse-echo system before (dotted lines for a zeroth-order beam, and dashed lines for second-order beams) and after (full lines) subtraction (absolute values).

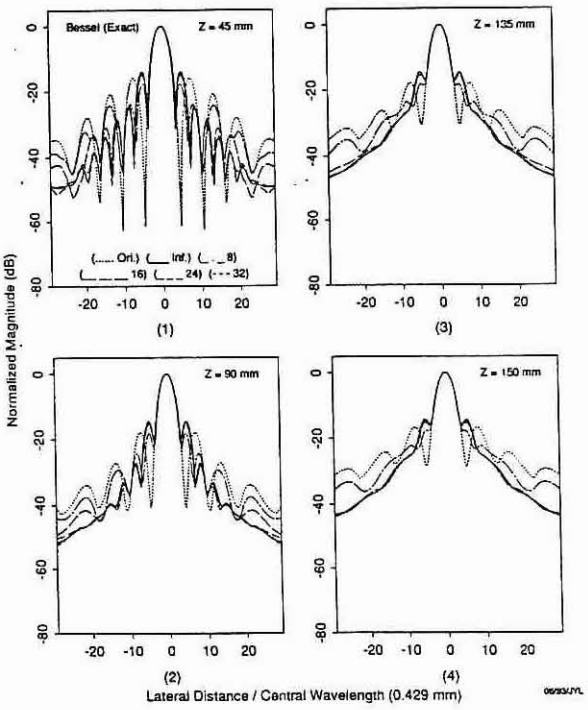

Fig. 3 Sidelobe reduction for a Bessel pulse-echo system when the transducer is weighted exactly along the radial distance and approximately along the angular direction. The vertical scale of the plots represents the maximum of the envelope of each A-line and plotted versus the radial distance. This gives the maximum sidelobes. The plots are obtained at 4 axial distances away from the transducer: (1) 45, (2) 90, (3) 135, and (4) 150 mm. Dotted lines represent sidelobes before subtraction. Full, dashed plus dotted, very long dashed, long dashed, and dashed lines represent sidelobes after subtraction with the transducer divided into infinite number of, 8, 16, 24, and 32 equally spaced sectors, respectively. The lateral axis is normalized to the central wavelength (0.429 mm) and the vertical axis is in the dB scale representing normalized magnitude.

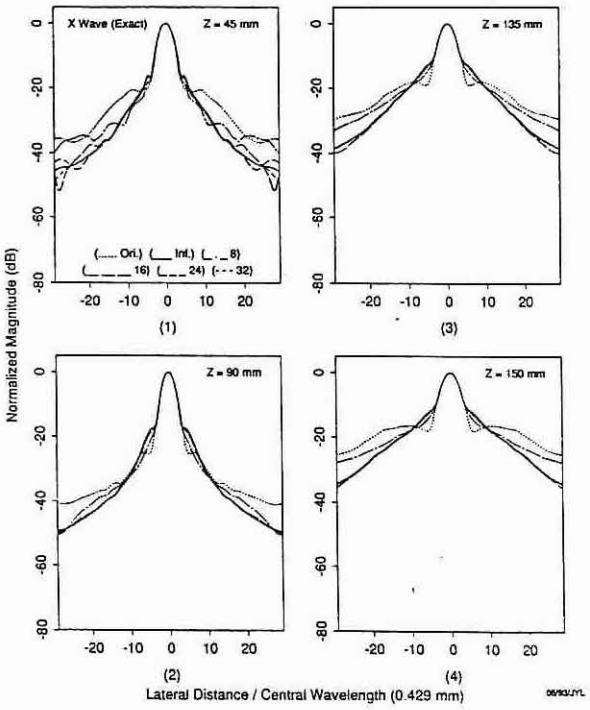

Fig. 4 Sidelobe reduction for an X wave pulse-echo system when the transducer is weighted exactly along the radial distance and approximately along the angular direction. The plots have the same format as that of Fig. 3.

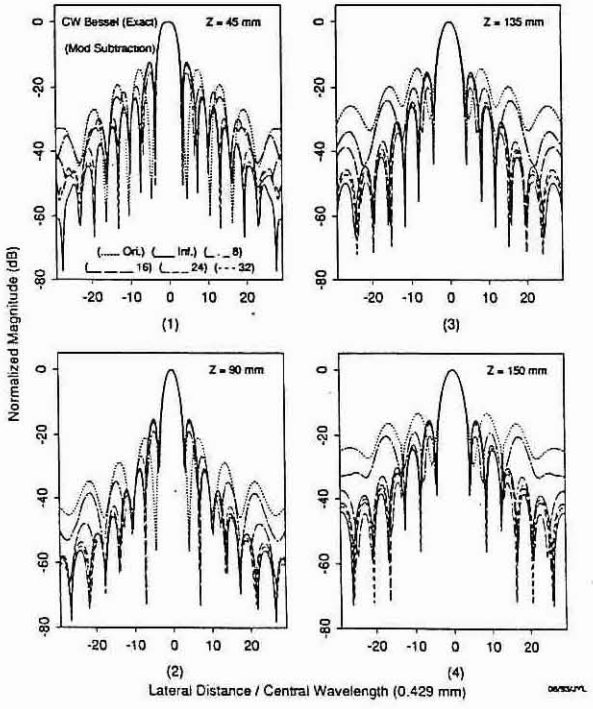

Fig. 5 Sidelobe reduction for the same Bessel pulse-echo system as that in Fig. 3, except that a long CW tone burst (3.5 MHz) is used to drive the transducer and the vertical scale of the plots represents the maximum of the envelope of the pulse-echo response along the angular direction from 0 to 2π and plotted versus the radial distance.

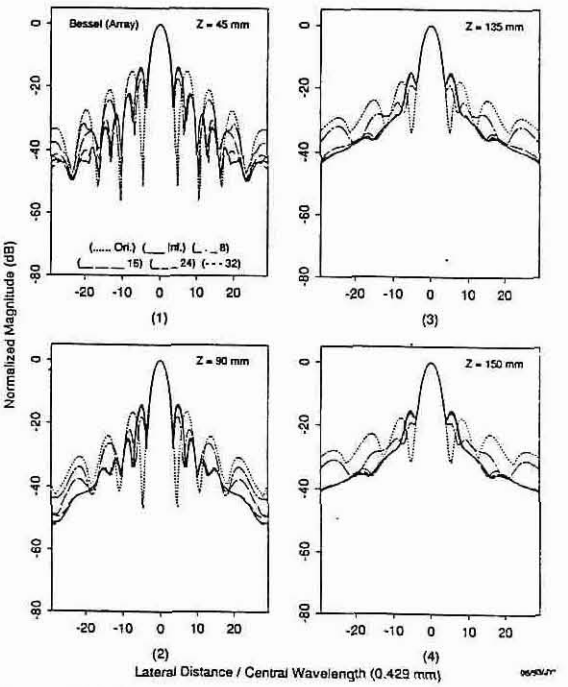

Fig. 6 Sidelobe reduction for a Bessel pulse-echo system when the transducer is weighted approximately with 14 rings along the radial distance and is also weighted approximately along the angular direction. The figure has the same format as that of Fig. 3.

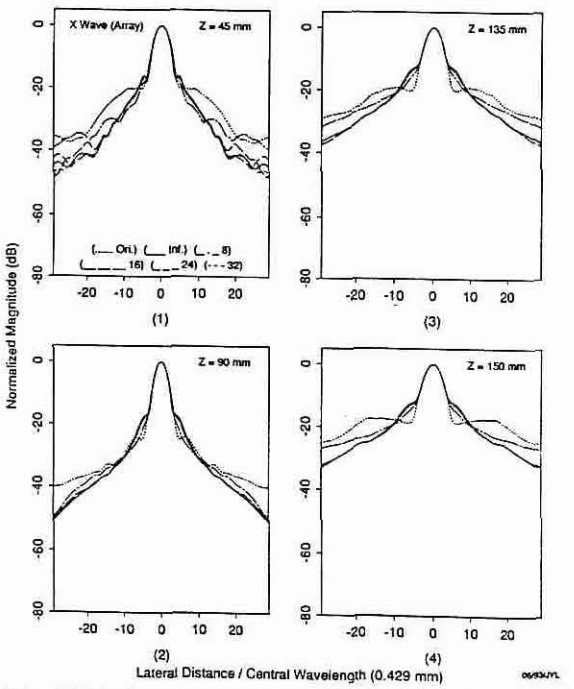

Fig. 7 Sidelobe reduction for an X wave pulse-echo system when the transducer is weighted approximately with 14 rings along the radial distance and is also weighted approximately along the angular direction. The figure has the same format as that of Fig. 4.

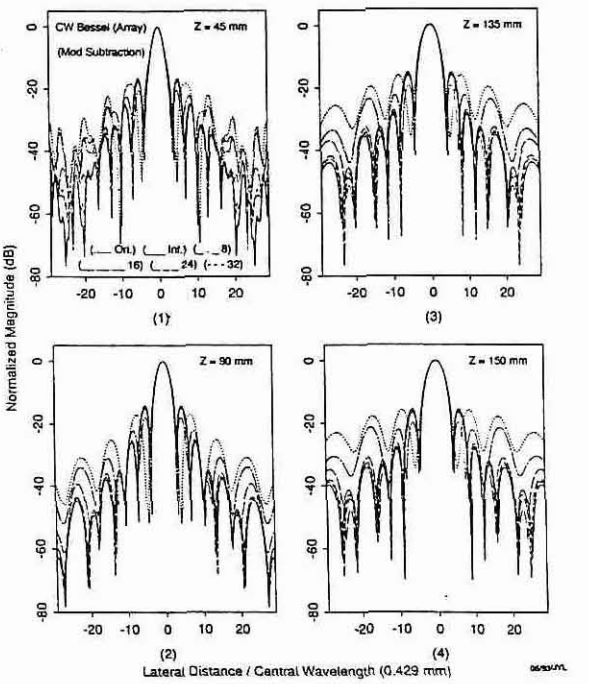

Fig. 8 Sidelobe reduction for the same Bessel pulse-echo system as that in Fig. 6, except that a long CW tone burst (3.5 MHz) is used to drive the transducer and the vertical scale of the plots represents the maximum of the envelope of the pulse-echo response along the angular direction from 0 to 2π and plotted versus the radial distance. The figure has the same format as that of Fig. 5.

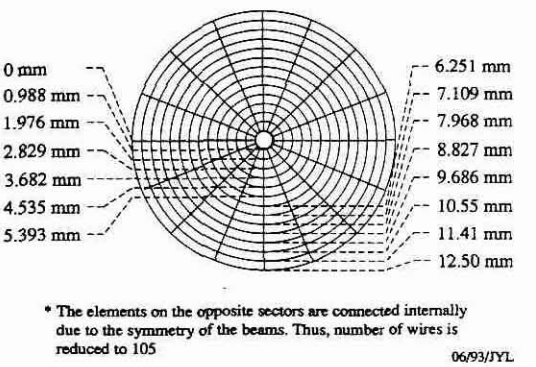

Fig. 9 A proposed transducer for producing both zeroth- and second-order limited diffraction beams and performing the summation-subtraction method to reduce the sidelobes. Apart from the 16 sectors, the transducer has the same structure as that we used in real-time medical imaging [16].